Mathematical Biosciences and Engineering

http://www.aimspress.com/journal/MBE

MBE, 18(1): 745–763.
DOI: 10.3934/mbe.2021040
Received: 03 October 2020
Accepted: 09 December 2020
Published: 18 December 2020

Research article

Noise-induced transitions in a non-smooth SIS epidemic model with media alert

Anji Yang[1], **Baojun Song**[2] **and Sanling Yuan**[1,*]

[1] College of Science, University of Shanghai for Science and Technology, Shanghai 200093, China
[2] Department of Applied Mathematics and Statistics, Montclair State University, Montclair, NJ 07043, USA

* **Correspondence:** Email: sanling@usst.edu.cn.

Abstract: We investigate a non-smooth stochastic epidemic model with consideration of the alerts from media and social network. Environmental uncertainty and political bias are the stochastic drivers in our mathematical model. We aim at the interfere measures assuming that a disease has already invaded into a population. Fundamental findings include that the media alert and social network alert are able to mitigate an infection. It is also shown that interfere measures and environmental noise can drive the stochastic trajectories frequently to switch between lower and higher level of infections. By constructing the confidence ellipse for each endemic equilibrium, we can estimate the tipping value of the noise intensity that causes the state switching.

Keywords: SIS model; media alert; noise-induced state switching; stochastic sensitivity; confidence domains

1. Introduction

These days have witnessed the horrible pandemic of COVID-19. As is known to the public, key characteristic of this killer is its silent spreads. Before we fully understand the virus, it has already established. In general, what do we do once a disease has invaded into a population? To mitigate the spread of a disease and eventually get a full control to the disease, the behavior changes at the population level can bend the infection curve. How to promote a massive behavior change? Two typical governing systems function differently. A central government can force a mandatory behavior change without any court challenge, period. If a mandatory preventive measure cannot be exercised or the administration failed to act following a scientific manner, media and social network are able to propagate the positive message in order to persuade behavior changes. A behavior change at the population level is highly media oriented. In fighting COVID-19 pandemic, WHO Director-General

Tedros Adhanom Ghebreyesus ever mentioned "We're not just fighting an epidemic; we're fighting an infodemic." For emerging and re-emerging epidemic diseases, research has shown that positive media coverage is an effective measure to control the diseases [1].

Massive media propagation and social network response to an epidemic take off only after an outbreak has been observed, so that the initial infection growth is following the regular epidemic process. The study here focuses on how to mitigate an epidemic through the awareness by media and social network. Media and social network response to an epidemic have to be based upon the number of known infected. That is, the pressure from media and social network impose to the population only until the prevalence reaches certain tipping point. We, therefore, will set up a cutting point for the number of infections, then let the media or the social network play its role in our model. A quick searching across the board of relevant literature, this question has been tackled mainly from the view of deterministic modeling. Scholars have proposed media functions to model the transmission rates [2–7]. For instance, Cui et al. [3] analyzed a susceptible-exposed-infected model by using $\beta(1 - e^{-mI})$ to characterize the effect of media coverage. Their results showed that weak media effects may not be helpful because the infections oscillate periodically. Misra et al. [8] formulated an SIS model to study the impact of awareness programs conducted by a media campaign on the spread of an infectious disease and showed that the spread of an infectious disease can be controlled by using awareness programs but the disease remains endemic due to immigration.

Research work in highlighting the role of media coverage and social media network without tipping point can be read in [2,3,5–7]. In reality, because of time delay and asymptotic infections, we consider that only when the number of infected individuals reaches a tipping value, the alerts and the pressure from media and social network can take place [9, 10]. Liu et al. [4] set a base line of infection (the tipping point) I_c to launch media alert. They consequently proposed a non-smooth but continuous transmission rate:

$$\beta(I) = \begin{cases} \beta, & 0 \le I \le I_c, \\ \beta\left(\frac{I_c}{I}\right)^p, & I > I_c, \end{cases} \tag{1}$$

where nonnegative constant p denotes the intensity of the media coverage. By assuming that the susceptible individuals follow the logistic growth and newborns directly enter into the susceptible class, they studied the following model:

$$\begin{cases} \dfrac{\mathrm{d}S}{\mathrm{d}t} = rS\left(1 - \dfrac{S}{a}\right) - \beta(I)IS + \gamma I, \\ \dfrac{\mathrm{d}I}{\mathrm{d}t} = \beta(I)IS - (d + \epsilon + \gamma)I, \end{cases} \tag{2}$$

where $S(t)$ and $I(t)$ are the sizes of susceptible and infectious population at time t, respectively. All parameters are positive. r is the intrinsic growth rate of the susceptible population; a is the carrying capacity of the community in the absence of infection; d denotes the natural death rate; γ represents the recovery rate of the infected individuals; ϵ is the disease-induced death rate. Liu et al. [4] conducted a rigorous and complete mathematical analysis to model (2).

Deterministic models always give us a good start to catch certain characteristic of a disease transmission. Obviously, these mean-field models are based upon the homogeneous population, uniform individual behavior, and steady environmental settings. In managing to fight an epidemic or pandemic infections, unexpected random factors also play a significant role. A certain false claims,

misinformation, conspiracy theories can change the course of epidemic. The rumors such as black people are immune to COVID-19 and coconut oil kills the virus of COVID-19 have misled some communities in battling the virus. Spreading false or misleading information may prevent the timely and effective adoption of appropriate behaviours and of public health recommendations or measures [11]. Occasional political bias or unusual unscientific statements can even create a temporal chaos in favor of the disease spread. In the real world, the transmissions of infectious diseases are inevitably affected by these unexpected factors. The variations of physical environmental factors [12], such as humidity, temperature, etc. can have a significant impact on the transmission of a disease. A well-known work was the experimental result of Lowen et al. [13].

The introduction of environmental noise into deterministic setup could exhibit unexpected behaviors which have no analogue in the deterministic models [14]. In the last few decades, researchers have done a lot of work regarding to this aspect [14–25]. In [24], a stochastically forced predator-prey model with environmental toxins was proposed to analyze the dynamical behavior of noise-induced transitions from coexistence to prey-only extirpation in the bistable zone. Nonlinear dynamical models can exhibit various new phenomena, such as stochastic resonance [26], noise-induced transitions [27], noise-induced ordering [28], noise-induced chaos [29], and noise-induced complexity [30]. Studies of the environmental noise effects on systems with multiple attractors have been steady growing [31]. Multi-stable systems of deterministic models can exhibit noise-induced state switching between deterministic attractors [32–35] when a noise is considered. Using the stochastic sensitivity functions (SSF), Bashkirtseva et al. [36] developed a new technique to construct the analytical description of stochastically forced equilibria and cycles of discrete-time models. In the present paper, we will use the SSF technique to explore the noise-induced state switching between two epidemic equilibria and estimate a threshold value of the noise intensity.

We organize this paper as following. In Section 2, we review the main results of deterministic model (2) and propose its stochastic counterpart. The studies of noise-induced transitions between two epidemic equilibria and construction of the confidence ellipses for equilibria will be presented in Section 3. Finally, we conclude our study by a simple discussion in Section 4.

2. Model formulation and the global existence and uniqueness of the solutions

We first briefly review the main results of deterministic model (2), then we study the corresponding stochastic counterpart.

2.1. A summary to the deterministic model

Notice that model (2) always exists two equilibria: the origin $O(0,0)$ and the disease-free equilibrium $E_0(a,0)$. The basic reproductive number is

$$R_0 = \frac{a\beta}{d+\epsilon+\gamma}. \tag{3}$$

Here, we highlight the interested results from [4], which will be directly used in the subsequent stochastic analysis.

Lemma 2.1. *If $R_0 < 1$, $E_0(a,0)$ is globally asymptotically stable. If $R_0 > 1$ together with certain extra conditions, in addition to saddles $O(0,0)$ and $E_0(a,0)$, there exist three endemic equilibria E_1,*

E_2 and E_3, where E_1 and E_3 are asymptotically stable and E_2 is a saddle. The separatrices (the stable manifolds of the saddle E_2) separate the domain of attractions of E_1 and E_3. Hence, bistable dynamics could be observed in model (2) *if* $R_0 > 1$.

In this paper, we pay more attentions to the epidemiological implications. Model (2) was set to investigate the media effects after the disease has already invaded the population. So the media alert and the pressure from social network have no impact to the initial growth of the disease. That is why the basic reproductive number R_0 is independent of the media alert parameters I_c and p. The appearance of the bistable dynamics is the straightforward outcome of the introduction of media impact. A bifurcation diagram is shown in Figure 1. It can be seen that model (2) undergoes a backward bifurcation at $R_0 \approx 4.8705$. There is a window $(4.3515, 4.8705)$ for R_0 where model (2) can have two stable equilibria E_1 and E_3 and a saddle E_2 (see also Figure 2 (a) where $\beta = 0.0139$). The appearance of the stable endemic state competing with the other stable endemic state is known as the bistability phenomenon. The media is helpful to interfare the infections by forcing (2) to choose smaller endemic E_1 as the attractor.

Table 1. Parameter values in numerical simulations for models (2).

Symbol	Description	Value range	Units
r	Intrinsic growth rate	1.35	year^{-1}
a	Carrying capacity of the community	700	None
d	Natural death rate	0.0133	year^{-1}
p	Intensity of the media effect on contact infection	3	None
ϵ	The disease-induced death rate	2	year^{-1}
β	Transmission rate	0.0087 – 0.0209	year^{-1}
γ	Recovered rate	0.0196	year^{-1}
I_c	The base line of infection to launch media alert	80	None

2.2. The stochastic model

In this paper we intend to explore the stochastic version of model (2). Stochastic factors such as the environmental noise, social noise, random misinformation spread though media and social network and political motivated biased information are not easy to handle with deterministic models. We integrate all these random factors into the deterministic model (2) to look into the following stochastic differential equation:

$$\begin{aligned} \mathrm{d}S &= \left[rS\left(1-\frac{S}{a}\right) - \beta(I)IS + \gamma I\right]\mathrm{d}t + \sigma_S S\,\mathrm{d}B_1, \\ \mathrm{d}I &= \left[\beta(I)IS - (d+\epsilon+\gamma)I\right]\mathrm{d}t + \sigma_I I\mathrm{d}B_2, \end{aligned} \tag{4}$$

where B_1 and B_2 are standard one-dimensional independent Brownian motions. We use σ_S and σ_I to denote the noise intensities. For the simplicity of discussion in this research, we assume $\sigma_S = \sigma_I = \sigma$.

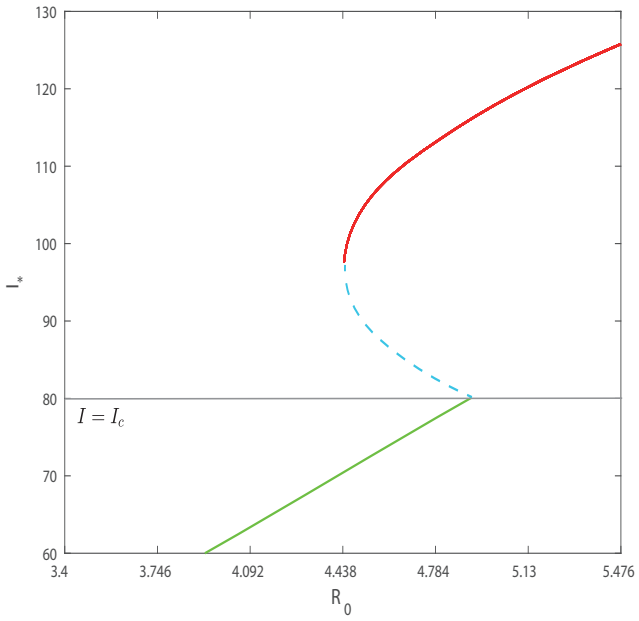

Figure 1. Bifurcation diagram when R_0 changes. Dashed line indicates unstable and solid stable. The selected parameter values are tabulated in Table 1.

Because system (4) is piecewise defined, we distinguish the noise intensities by $\sigma = \sigma_1$ when $I > I_c$ and $\sigma = \sigma_2$ when $I \leq I_c$.

2.3. Global existence and uniqueness of solutions

Since we are more interested in the asymptotic behavior of the model, we first anticipate that all solutions exist for all forward times. Now we prove the existence and uniqueness of the global positive solution of stochastic model (4).

Theorem 2.2. *For any given positive initial value* $(S(0), I(0)) \in \Re^2_+$*, model* (4) *has a unique positive solution* $(S(t), I(t))$ *for* $t \geq 0$*. Moreover, the solution will remain in* $\Re^2_+$ *with probability one, namely,* $(S(t), I(t)) \in \Re^2_+$ *for all* $t \geq 0$ *almost surely (a.s.).*

Proof. Without loss of generality, we assume that $I(0) > I_c$. Let us introduce the stopping time sequence $\{\tau_i\}, i = 1, 2, \cdots$ as follows:

$$\tau_1 = \inf\{t \geq 0, I(t) \leq I_c\}, \qquad \tau_2 = \inf\{t \geq \tau_1, I(t) > I_c\}$$

and

$$\tau_{2n+1} = \inf\{t \geq \tau_{2n}, I(t) \leq I_c\}, \qquad \tau_{2n+2} = \inf\{t \geq \tau_{2n+1}, I(t) > I_c\}$$

for $n = 1, 2, \cdots$. Thus when $t \in [\tau_{2n}, \tau_{2n+1})$, model (4) becomes

$$\begin{aligned} \mathrm{d}S &= \left[rS\left(1 - \frac{S}{a}\right) - \beta\left(\frac{I_c}{I}\right)^p IS + \gamma I\right]\mathrm{d}t + \sigma_1 S\,\mathrm{d}B_1, \\ \mathrm{d}I &= \left[\beta\left(\frac{I_c}{I}\right)^p IS - (d + \epsilon + \gamma)I\right]\mathrm{d}t + \sigma_1 I\mathrm{d}B_2, \end{aligned} \tag{5}$$

and when $t \in [\tau_{2n+1}, \tau_{2n+2})$, model (4) becomes

$$\begin{aligned} \mathrm{d}S &= \left[rS\left(1-\frac{S}{a}\right) - \beta IS + \gamma I\right]\mathrm{d}t + \sigma_2 S\,\mathrm{d}B_1, \\ \mathrm{d}I &= \left[\beta IS - (d+\epsilon+\gamma)I\right]\mathrm{d}t + \sigma_2 I\mathrm{d}B_2, \end{aligned} \tag{6}$$

where $n = 0, 1, 2, \cdots$ and $\tau_0 = 0$. Notice that (5) and (6) both have a unique global positive solution for any initial value $(S(0), I(0)) \in \mathfrak{R}^2_+$. This implies model (4) has a unique local positive solution $(S(t), I(t))$ on $[0, \tau_e)$, where τ_e is the explosion time. In order to prove the solution is global, we only need to prove $\tau_e = \infty$, *a.s.*

Let $k_0 > 0$ be sufficiently large such that $S(0)$ and $I(0)$ both lie within the interval $\left[\frac{1}{k_0}, k_0\right]$. For all integer $k > k_0$, we define the stopping time

$$\tilde{\tau}_k = \inf\left\{t \in [0, \tau_e) : \min\{S(t), I(t)\} \le \frac{1}{k} \text{ or } \max\{S(t), I(t)\} \ge k\right\}.$$

Clearly, $\tilde{\tau}_k$ is an increasing function as $k \to \infty$. Let $\tilde{\tau}_\infty = \lim_{k\to\infty} \tilde{\tau}_k$, whence $\tilde{\tau}_\infty \le \tau_e$, *a.s.* If we can prove $\tilde{\tau}_\infty = \infty$, then $\tau_e = \infty$, and $(S(t), I(t)) \in \mathfrak{R}^2_+$ for all $t \ge 0$, *a.s.* Hence, we only need to show that $\tilde{\tau}_\infty = \infty$, *a.s.* We prove this by contradiction. If this assertion is false, then there exists a pair of constants $T > 0$ and $\varepsilon \in (0, 1)$ such that $P\{\tilde{\tau}_\infty \le T\} > \varepsilon$, hence there exists $k_1 > k_0$ such that

$$P\{\tilde{\tau}_k \le T\} \ge \varepsilon \tag{7}$$

for all $k \ge k_1$. Define a nonnegative C^2-function $V : \mathfrak{R}^2_+ \to \mathfrak{R}_+$ by

$$V(S, I) = S - m - m\ln\frac{S}{m} + I - 1 - \ln I,$$

where $m = \frac{d+\epsilon}{\beta}$. Applying Itô's formula, we obtain respectively from (5) and (6) that for $t \in [\tau_{2n}, \tau_{2n+1})$,

$$\mathrm{d}V(S, I) = \mathrm{L}V(S, I)\mathrm{d}t + \sigma_1(S - m)\mathrm{d}B_1 + \sigma_1(I - 1)\mathrm{d}B_2,$$

where

$$\begin{aligned} \mathrm{L}V(S, I) =& \left(1 - \frac{m}{S}\right)\left[rS\left(1-\frac{S}{a}\right) - \beta\left(\frac{I_c}{I}\right)^p IS + \gamma I\right] \\ &+ \left(1 - \frac{1}{I}\right)\left[\beta\left(\frac{I_c}{I}\right)^p IS - (d+\epsilon+\gamma)I\right] + \frac{1}{2}m\sigma_1^2 + \frac{1}{2}\sigma_1^2 \\ \le& r\left(1+\frac{m}{a}\right)S - \frac{r}{a}S^2 + (m\beta - d - \epsilon)I + (d+\epsilon+\gamma) + \frac{1}{2}m\sigma_1^2 + \frac{1}{2}\sigma_1^2 \\ \le& r\left(1+\frac{m}{a}\right)S - \frac{r}{a}S^2 + (d+\epsilon+\gamma) + \frac{1}{2}m\sigma_1^2 + \frac{1}{2}\sigma_1^2 < M_1, \end{aligned}$$

and that for $t \in [\tau_{2n+1}, \tau_{2n+2})$,

$$\mathrm{d}V(S, I) = \mathrm{L}V(S, I)\mathrm{d}t + \sigma_2(S - m)\mathrm{d}B_1 + \sigma_2(I - 1)\mathrm{d}B_2,$$

where

$$\begin{aligned}\mathrm{L}V(S,I) =& \left(1-\frac{m}{S}\right)\left[rS\left(1-\frac{S}{a}\right)-\beta IS+\gamma I\right]\\ &+\left(1-\frac{1}{I}\right)[\beta IS-(d+\epsilon+\gamma)I]+\frac{1}{2}m\sigma_2^2+\frac{1}{2}\sigma_2^2\\ \leq& r\left(1+\frac{m}{a}\right)S-\frac{r}{a}S^2+(d+\epsilon+\gamma)+\frac{1}{2}m\sigma_2^2+\frac{1}{2}\sigma_2^2<M_2,\end{aligned}$$

where M_1 and M_2 are two positive numbers. Therefore, we have that for $t\in[\tau_{2n},\tau_{2n+1})$,

$$\mathrm{d}V(S,I)\leq M_1\mathrm{d}t+\sigma_1(S-m)\mathrm{d}B_1+\sigma_1(I-1)\mathrm{d}B_2 \tag{8}$$

and that for $t\in[\tau_{2n+1},\tau_{2n+2})$,

$$\mathrm{d}V(S,I)\leq M_2\mathrm{d}t+\sigma_2(S-m)\mathrm{d}B_1+\sigma_2(I-1)\mathrm{d}B_2. \tag{9}$$

Without loss of generality, we assume that $(\tilde{\tau}_k\wedge T)\in[\tau_{2m},\tau_{2m+1})$ for some $n=m$ (same logic follows when $(\tilde{\tau}_k\wedge T)\in[\tau_{2m+1},\tau_{2m+2})$). This together with (8) and (9) yields

$$\begin{aligned}&V(S(\tilde{\tau}_k\wedge T),I(\tilde{\tau}_k\wedge T))\\ \leq& V(S(0),I(0))+\sum_{n=0}^{m-1}\left(\int_{\tau_{2n}}^{\tau_{2n+1}}M_1\mathrm{d}t+\int_{\tau_{2n}}^{\tau_{2n+1}}\sigma_1(S-m)\mathrm{d}B_1+\int_{\tau_{2n}}^{\tau_{2n+1}}\sigma_1(I-1)\mathrm{d}B_2\right)\\ &+\sum_{n=0}^{m-1}\left(\int_{\tau_{2n+1}}^{\tau_{2n+2}}M_2\mathrm{d}t+\int_{\tau_{2n+1}}^{\tau_{2n+2}}\sigma_2(S-m)\mathrm{d}B_1+\int_{\tau_{2n+1}}^{\tau_{2n+2}}\sigma_2(I-1)\mathrm{d}B_2\right)\\ &+\int_{\tau_{2m}}^{\tilde{\tau}_k\wedge T}M_1\mathrm{d}t+\int_{\tau_{2m}}^{\tilde{\tau}_k\wedge T}\sigma_1(S-m)\mathrm{d}B_1+\int_{\tau_{2m}}^{\tilde{\tau}_k\wedge T}\sigma_1(I-1)\mathrm{d}B_2.\end{aligned}$$

Taking the expectations on both sides of the above inequality leads to

$$\mathrm{E}V(S(\tilde{\tau}_k\wedge T),I(\tilde{\tau}_k\wedge T))\leq V(S(0),I(0))+M\mathrm{E}(\tilde{\tau}_k\wedge T),$$

where $M=\max\{M_1,M_2\}$. Thus

$$\mathrm{E}V(S(\tilde{\tau}_k\wedge T),I(\tilde{\tau}_k\wedge T))\leq V(S(0),I(0))+MT. \tag{10}$$

Let $\Omega_k=\{\omega\in\Omega:\tilde{\tau}_k=\tilde{\tau}_k(\omega)\leq T\}$ for $k\geq k_1$ and, by (7), $P\{\Omega_k\}\geq\varepsilon$. Note that for every $\omega\in\Omega_k$, we have either $S(\tilde{\tau}_k,\omega)$ or $I(\tilde{\tau}_k,\omega)$ equals either k or $\frac{1}{k}$. Hence $V(S(\tilde{\tau}_k,\omega),I(\tilde{\tau}_k,\omega))$ is no less than either

$$\left(k-m-m\ln\frac{k}{m}\right)\wedge(k-1-\ln k)\quad\text{or}\quad\left(\frac{1}{k}-m+m\ln km\right)\wedge\left(\frac{1}{k}-1+\ln k\right),$$

where "$a\wedge b$" means "the smaller one of a and b". It then follows from (10) that

$$\begin{aligned}&V(S(0),I(0))+MT\\ \geq&\mathrm{E}[I_{\Omega_k}V(S(\tilde{\tau}_k,\omega),I(\tilde{\tau}_k,\omega))]\end{aligned}$$

$$\geq \varepsilon \left[\left(k - m - m \ln \frac{k}{m} \right) \wedge (k - 1 - \ln k) \wedge \left(\frac{1}{k} - m + m \ln km \right) \wedge \left(\frac{1}{k} - 1 + \ln k \right) \right],$$

where I_{Ω_k} is the indicator function of Ω_k. Letting $k \to \infty$ we have

$$\infty > V(S(0), I(0)) + MT = \infty,$$

a contradiction. So we must have $\tau_\infty = \infty$, *a.s.* This completes the proof. □

In the following, we study the phenomenon of noise-induced transitions between two stochastic attractors for stochastic model (4).

3. Analysis of noise-induced transitions

In this section, the phenomenon of noise-induced transitions between two endemic equilibria is studied by constructing confidence ellipses with the technique of stochastic sensitivity functions (SSF).

We take the parameter values in Table 1 and set $I_c = 80$. The three endemic equilibria for model (2) are $E_1 = (146.2542, 77.3821)$, $E_2 = (159.3644, 82.3223)$, $E_3 = (413.8380, 113.1525)$. In Figure 2, phase plane of the deterministic model with parameters in Table 1 is shown, where the red-dotted curve Γ (the stable manifold of E_2) is the separatrix of two basins of attraction and the gray one ($I = I_c$) is the separatrix of two subsystems. As one can see, for the deterministic model, the trajectories with initial value inside of Γ tend to E_1, and the trajectories with initial value outside of Γ approach E_3.

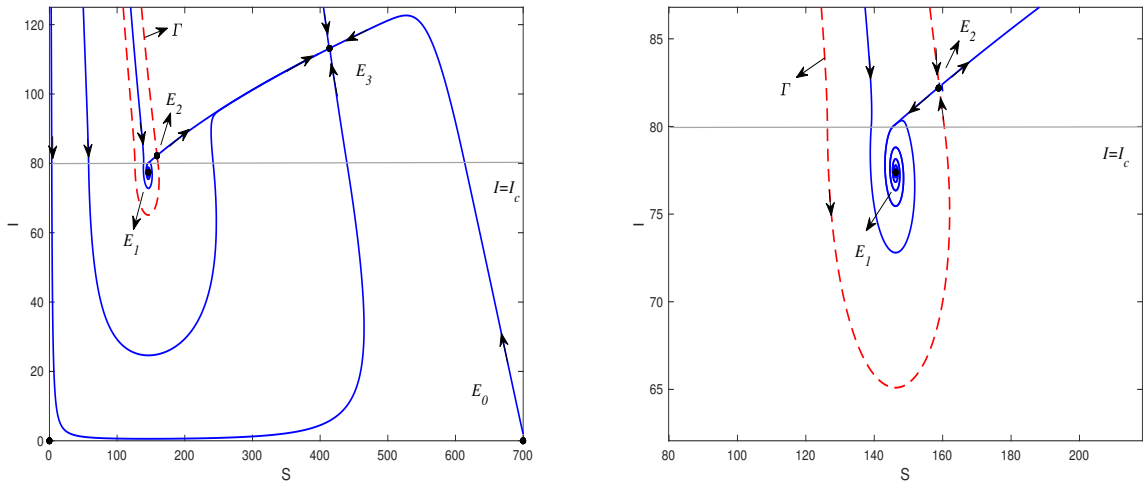

Figure 2. Phase plane (a) of the non-smooth model (2) with parameters in Table 1. (b) is a local enlarged view of (a).

For the stochastic model, we take endemic equilibria E_3 as an example. It is worth noting that endemic equilibria E_3 is located above the threshold I_c. When the noise intensity is small, here, we take $\sigma_1 = 0.1$, the stochastic trajectories with initial value near E_3 will hover around it (see Figure 3). However, as the noise intensity increases ($\sigma_1 = 0.25$), the steady state switches from high epidemic

E_3 to low epidemic E_1 (see Figure 4). It is also observed that the noise-induced transitions from low epidemic E_1 to high epidemic E_3.

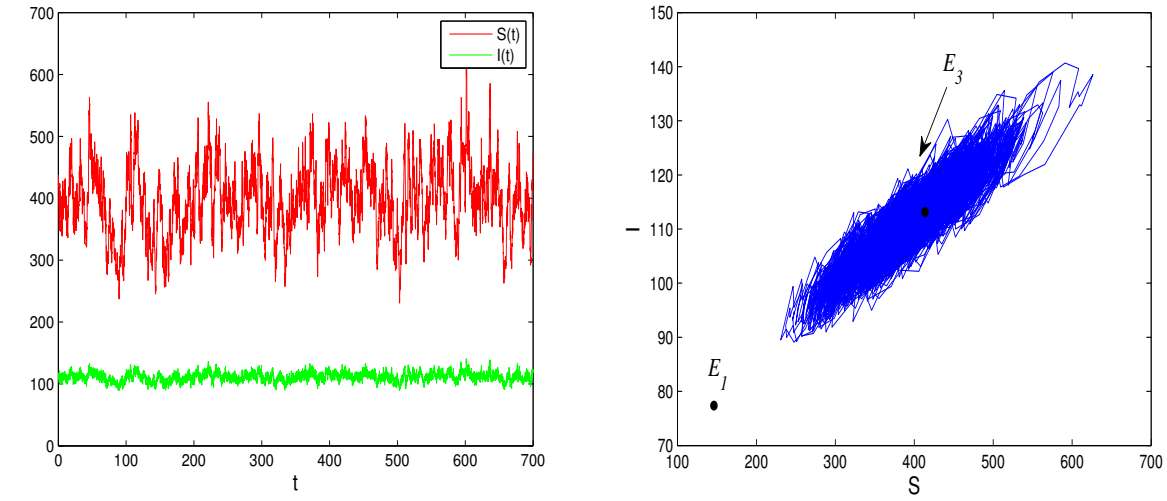

(a) (b)

Figure 3. Time series (a) of $S(t)$ and $I(t)$; Phase trajectory (b) for stochastic model (4) with initial value $(413, 113)$ and noise intensity $\sigma_1 = 0.1$.

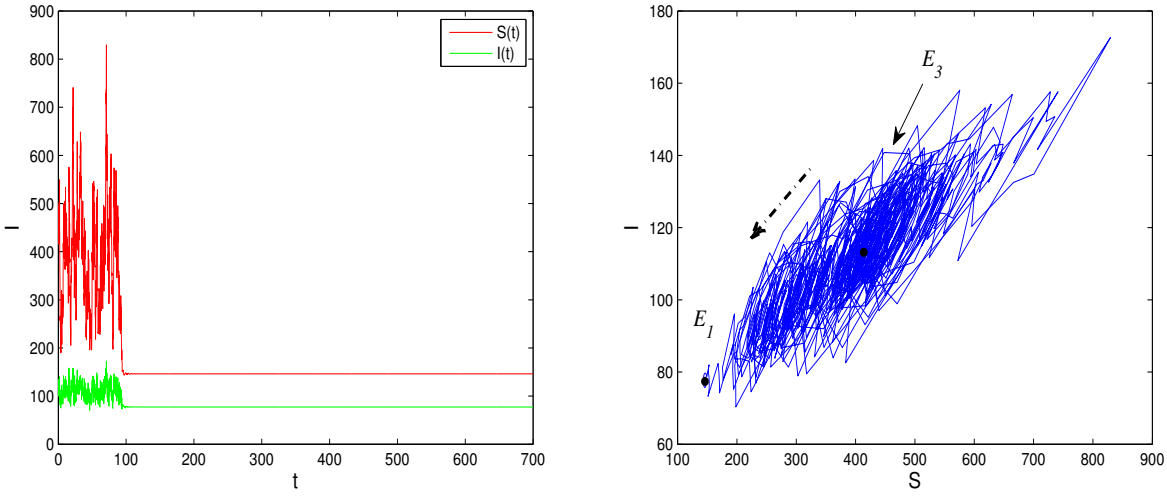

(a) (b)

Figure 4. Time series (a) of $S(t)$ and $I(t)$; Phase trajectory (b) for stochastic model (4) with initial value $(413, 113)$ and noise intensity $\sigma_1 = 0.25$.

3.1. Noise-induced state frequent switching

In the following, we construct confidence ellipses for stochastic model (4) by applying the stochastic sensitivity function technique (see the Appendix in [37]). We then further estimate the critical value of

the noise intensity that causes state switching.

For an endemic equilibrium $\bar{E} = (\bar{S}, \bar{I})$ of deterministic model (2), let $F = \begin{pmatrix} f_{11} & f_{12} \\ f_{21} & f_{22} \end{pmatrix}$ be the Jacobian matrix of (f, g) with respect to (S, I) at $\bar{E}$, where

$$\begin{aligned} f_{11} &= r(1 - \frac{2}{a}\bar{S}) - \beta(\bar{I})\bar{I}, \\ f_{12} &= -\beta'(\bar{I})\bar{S}\,\bar{I} - \beta(\bar{I})\bar{S} + \gamma, \\ f_{21} &= \beta(\bar{I})\bar{I}, \\ f_{22} &= \beta'(\bar{I})\bar{S}\,\bar{I} + \beta(\bar{I})\bar{S} - (d + \epsilon + \gamma), \end{aligned}$$

We define $g_{11} = \bar{S}$, $g_{22} = \bar{I}$, and $G = \begin{pmatrix} g_{11} & 0 \\ 0 & g_{22} \end{pmatrix}$. After solving the following system of linear equations for $w_{ij}, i, j = 1, 2$,

$$\begin{cases} 2f_{11}w_{11} + f_{12}w_{12} + f_{12}w_{21} = -g_{11}^2, \\ f_{21}w_{11} + (f_{11} + f_{22})w_{12} + f_{12}w_{22} = 0, \\ f_{21}w_{11} + (f_{11} + f_{22})w_{21} + f_{12}w_{22} = 0, \\ f_{21}w_{12} + f_{21}w_{21} + 2f_{22}w_{22} = -g_{22}^2, \end{cases}$$

we obtain the stochastic sensitivity matrix $W = \begin{pmatrix} w_{11} & w_{12} \\ w_{21} & w_{22} \end{pmatrix}$. Given that a noise intensity $\bar{\sigma}$ and a fiducial probability P, then applying the formula A.3 from [37] we obtain the confidence ellipse equation for the equilibrium $\bar{E} = (\bar{S}, \bar{I})$

$$\left\langle (S - \bar{S}, I - \bar{I})^T, W^{-1}((S - \bar{S}, I - \bar{I})^T) \right\rangle = 2\bar{\sigma}^2 \ln \frac{1}{1 - P}. \tag{11}$$

Applying (11) to $E_3 = (413.8380, 113.1525)$, the corresponding stochastic sensitivity matrix and its inverse are

$$W = \begin{pmatrix} 194704.7876 & 17235.9757 \\ 17235.9757 & 2620.5725 \end{pmatrix} \text{ and } W^{-1} = \begin{pmatrix} 0.000012 & -0.000081 \\ -0.000081 & 0.0009134 \end{pmatrix}.$$

The confidence ellipse equation of E_3 is

$$1.2{\cdot}10^{-5}{\cdot}(S-413.838)^2 - 1.6{\cdot}10^{-4}{\cdot}(S-413.838)(I-113.1525) + 9.1{\cdot}10^{-4}{\cdot}(I-113.1525)^2 = 2\sigma_1^2 \ln \frac{1}{1-P}.$$

Fixing fiducial probability $P = 0.95$, we next observe how different intensity noise affects the confidence ellipse. When $\sigma_1 = 0.1$, the corresponding stochastic states and confidence ellipses of subsystem (5) are shown in Figure 5. As shown in the figure, the random states of the stochastic model are distributed around the deterministic endemic equilibrium E_3, and located inside of the confidence ellipses with probability 0.95.

We then take two larger noise intensities $\sigma_1 = 0.24$ and $\sigma_1 = 0.28$, the corresponding confidence ellipses are shown in Figure 6. As the noise intensity increases, the confidence ellipse is growing. It

crosses separatrix Γ (the stable manifold of E_2) and ultimately arrives at the domain of attraction of the low endemic equilibrium E_1. The noise intensity value that corresponds to the confidence ellipse intercepts with Γ can be regarded as the critical noise intensity $\hat{\sigma}_1$. Here $\hat{\sigma}_1 \approx 0.24$. A typical example that the trajectory of stochastic model (4) starting near the endemic equilibrium E_3 converges to the other endemic equilibrium E_1 is shown in Figure 4 in which $\sigma_1 = 0.25 > \hat{\sigma}_1$.

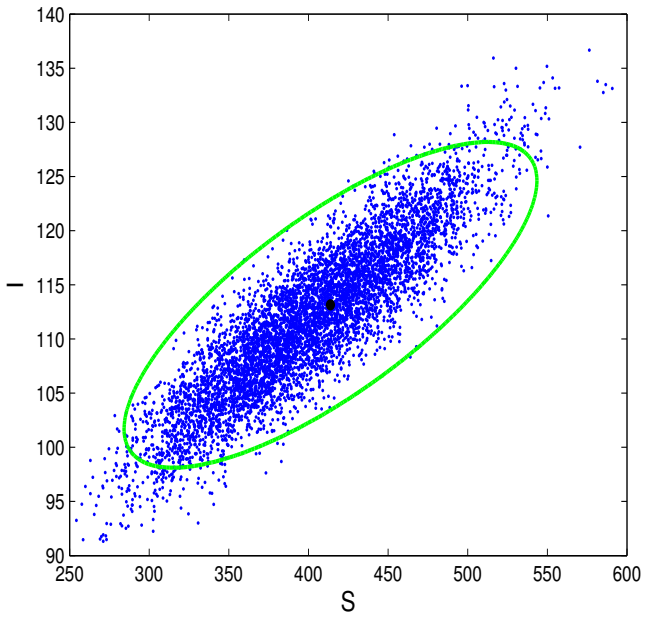

Figure 5. Random states (blue) of stochastic model (5) and confidence ellipse (green) for $\sigma_1 = 0.1$.

Next we construct the confidence ellipse for E_1. The corresponding stochastic sensitivity matrix and its inverse of endemic equilibrium E_1 are

$$W = \begin{pmatrix} 55873.2322 & -2783.5288 \\ -2783.5288 & 30253.2528 \end{pmatrix} \text{ and } W^{-1} = \begin{pmatrix} 0.000018 & 0.0000017 \\ 0.0000017 & 0.000033 \end{pmatrix}.$$

The corresponding equation of the confidence ellipse for E_1 is

$$1.8{\cdot}10^{-5}{\cdot}(S-146.2542)^2+3.3{\cdot}10^{-6}{\cdot}(S-146.2542)(I-77.3821)+3.3{\cdot}10^{-5}{\cdot}(I-77.3821)^2 = 2\sigma_2^2 \ln\frac{1}{1-P}.$$

Putting the confidence ellipses for E_1 and E_3 together can give us a better looking of the whole system. For weaker noise ($\sigma_1 = 0.1, \sigma_2 = 0.02$), confidence ellipses of both E_1 (green) and E_3 (blue) are located inside their own attraction basin. They are distinctly separated by the separatrix Γ (in red) (see Figure 7 (a)). The random trajectories starting from inside of the separatrix will fluctuate around the endemic equilibrium E_1, and the ones starting from outside of the separatrix will fluctuate around the endemic equilibrium E_3. The random trajectories leaving the unforced deterministic attractors concentrate in their small neighborhoods (see Figure 7 (c)). One can see the weaker noise does not affect the dynamics of the stochastic model (4).

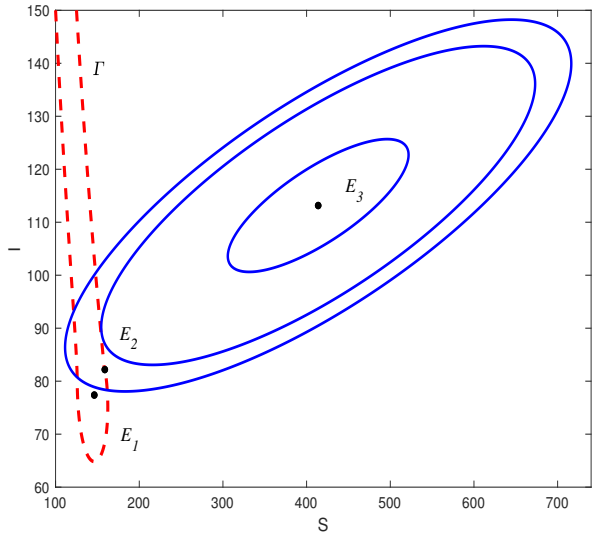

Figure 6. Separatrix (red dashed) and confidence ellipses (blue solid) for $\sigma_1 = 0.1$ (small), $\sigma_1 = 0.24$ (middle), $\sigma_1 = 0.28$ (large).

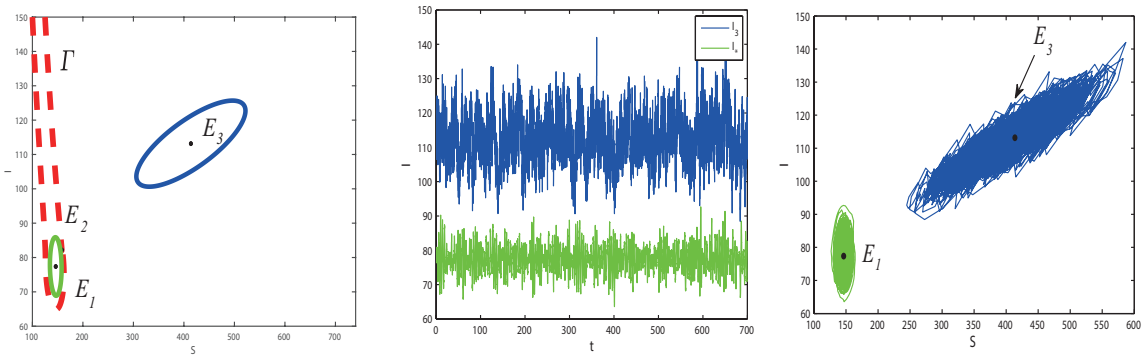

Figure 7. Confidence ellipses (a), time series (b), and random trajectories (c) for stochastic model (4) when $\sigma_1 = 0.1$ and $\sigma_2 = 0.02$.

We fix $\sigma_2 = 0.02$ and increase σ_1 to 0.28, then the confidence ellipse (blue) of E_3 crosses the separatrix (see Figure 8 (a)). The stochastic trajectories starting within the attraction basin of E_3 will cross the separatrix and approach E_1 with high probability (see Figure 8 (c)). This is also shown by the time series (see Figure 8 (b)): the number of infected cases ultimately is stabilized around I_1 (a smaller value). To better understand this, we numerically obtain the stationary probability density (SPD) of model (4). In Figure 8 (d), we can see that the SPD for stochastic model (4) has a maximum value at I_1, which implies that the sample trajectory will stay for a longer time in the neighborhood of I_1. In other words, I_1 is stable in the meaning of probability (with a bigger probability). This illustrates that the phenomenon of noise-induced transition occurs as the noise intensity σ_1 increases.

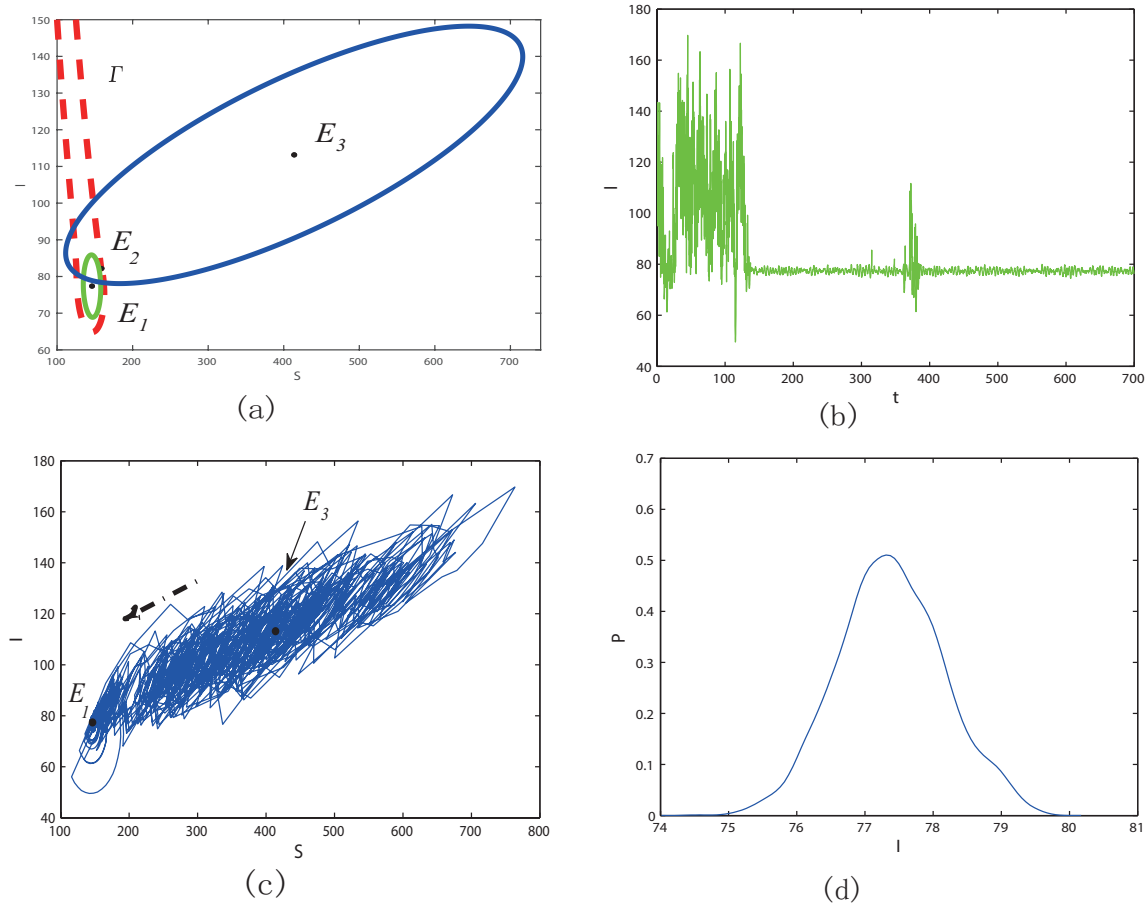

Figure 8. Confidence ellipses (a), time series (b), random trajectory (c), and stationary probability density (d) for stochastic model (4) with initial value $(413, 113)$ and noise intensity $\sigma_1 = 0.28$, $\sigma_2 = 0.02$.

We also obtain a symmetric result by fixing $\sigma_1 = 0.1$ and increasing σ_2 to 0.04 (see Figure 9). In this scenario, the confidence ellipse of E_1 crosses the separatrix Γ. That is, the number of infected cases ultimately maybe jump to I_3 (a bigger value), thus making the infections worse.

Finally, we let both intensities change, increasing σ_1 to 0.28 and σ_2 to 0.04. As expected that the phenomenon of frequent random hopping occur between two attractors E_1 and E_3 is observed. We can see from Figure 10 (a) that both the two confidence ellipses of E_1 and E_3 cross the separatrix Γ,

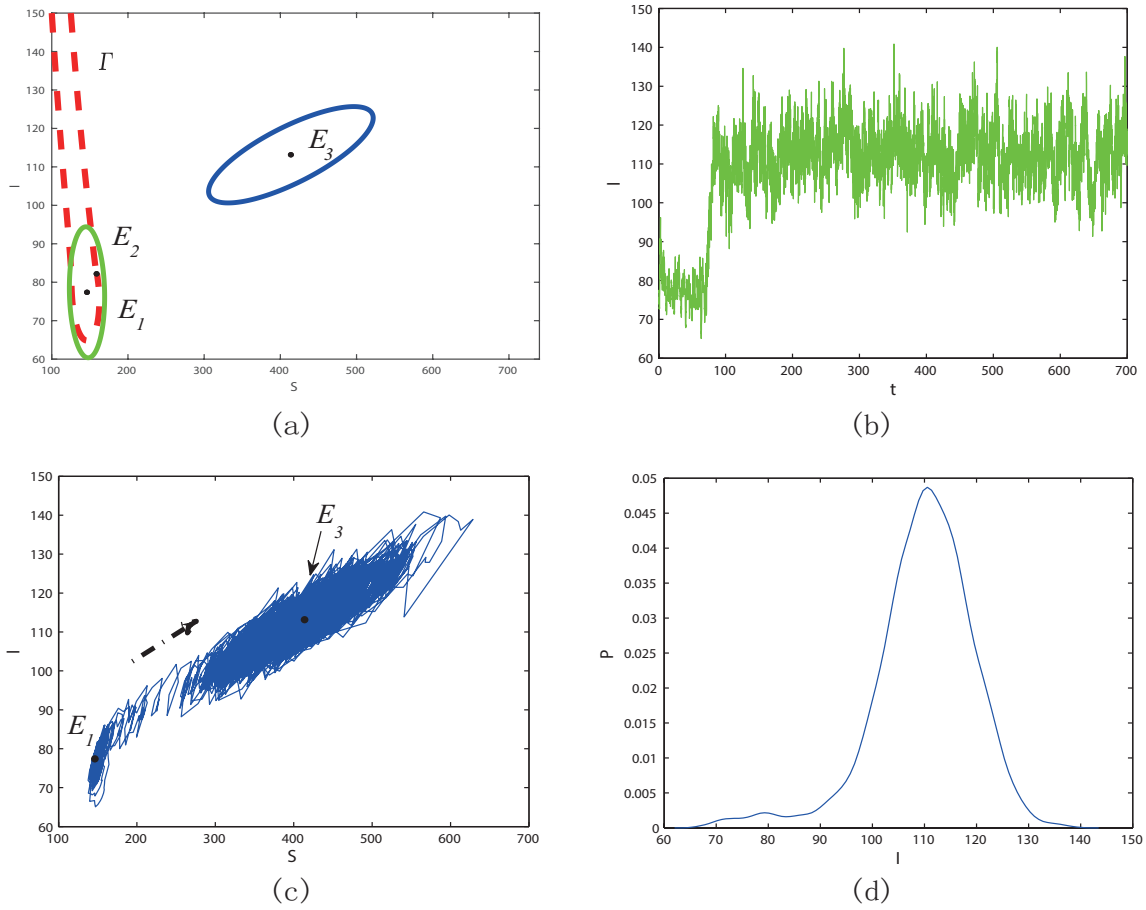

Figure 9. Confidence ellipses (a), time series (b), random trajectory (c), and stationary probability density (d) for stochastic model (4) with initial value (146, 77) and noise intensity $\sigma_1 = 0.1, \sigma_2 = 0.04$.

and the region that the two confidence ellipses intersect builds a "transition bridge" between basins of attraction. In this overlapped region, noise-induced transitions can occur with greater probability (see Figure 10 (b) and (c)). In addition, we can also see from Figure 10 (d) that the SPD for stochastic model (4) has two maximum value at I_1 and I_3. In this case, stochastic force can worse the picture of infection, it can also mitigate an infection.

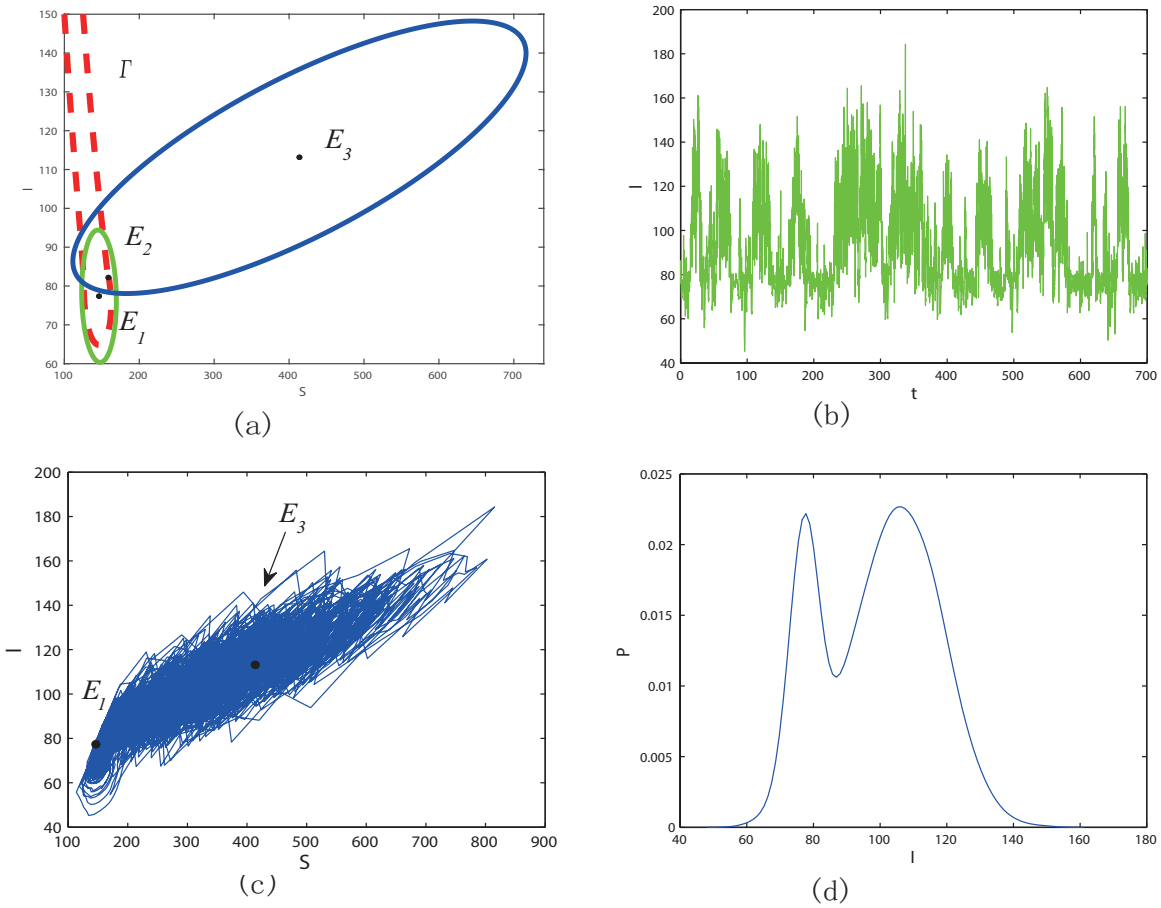

Figure 10. Confidence ellipses (a), time series (b), random trajectory (c), and stationary probability density (d) for stochastic model (4) with initial value (146, 77) and noise intensity $\sigma_1 = 0.28$, $\sigma_2 = 0.04$.

4. Discussion

What do we do "if the horse has left the barn"? We are still optimistic. Never too late to take an action. Scientific oriented media alert and positive energy spread over the social network are able to guide us walking out of the woods. For epidemics associated with emerging and re-emerging infectious diseases, we can bend the infection curve if we are oriented scientifically. We can smartly use the media coverage and social network to help us to fight an epidemic. Using mathematical model we have shown that alerts from media and/or social network play an important role in the battle of fighting the disease spread.

The final size of the epidemic depends on the media and social network coverage parameters p and I_c. A clear monotonic patten of the final size can be seen shown in Figure 11 (a). Under the same noise intensity (we set $\sigma_1 = 0.005$), the greater the media and social network coverage, the smaller the final size. The same monotonic patten is observed in Figure 11 (b), the final infection scale decreases when the threshold I_c decreases. This suggests that the decision makers should set appropriate threshold I_c to minimise the infection scale.

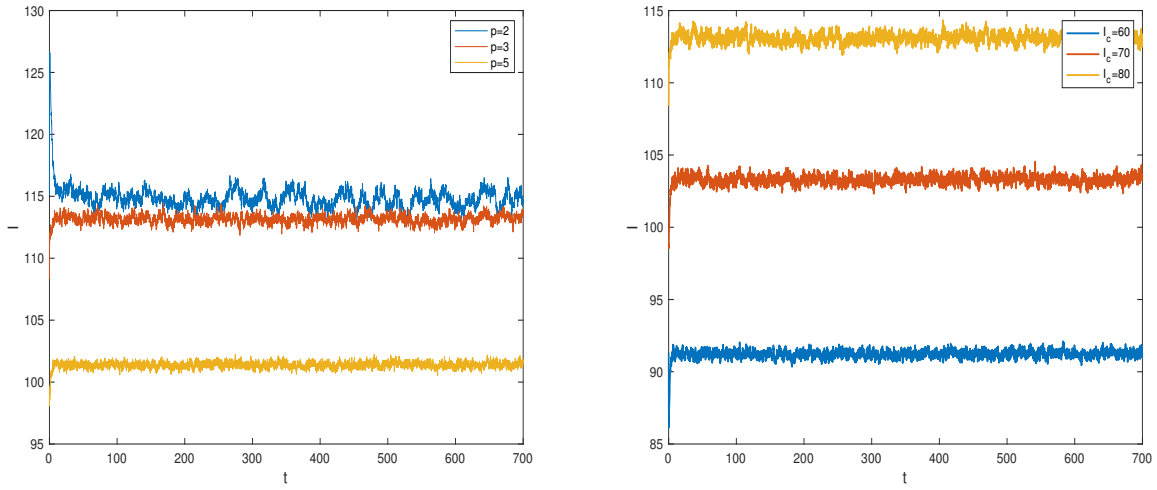

(a) (b)

Figure 11. Time series of $I(t)$ for stochastic model (4) with same noise intensity $\sigma_1 = 0.005$ and different (a) intensity of media coverage p, (b) threshold number of infected I_c.

Since the alerts from media social network are triggered only after an initial epidemic, it does reduce the magnitude of the infection. However, one cannot overstate its role in containing an epidemic, mainly because these alerts do not modify the basic reproductive number. It is out of the reach of these alerts to bring the basic reproductive number less than one.

The magnitude of a confidence ellipse is proportional to the intensity of the noise. The bigger the noise, the bigger the corresponding confidence ellipse. Then we are sure that intensifying the noise will raise the likelihood of endemic state shift. However, in terms steady state mobile attributed to the noise, current model cannot distinguish whether it bring the epidemic downward or upward.

Acknowledgments

We are very grateful to both the editor and the reviewers for their valuable comments and suggestions, which have greatly improved the quality and presentation of our paper. This work was supported by the National Natural Science Foundation of China (11671260; 12071293).

Conflict of interest

The authors declare there is no conflict of interest.

References

1. M. S. Rahman, M. L. Rahman, Media and education play a tremendous role in mounting aids awareness among married couples in bangladesh, *AIDS Res. Ther.*, **4** (2007), 1–7.
2. J. Cui, X. Tao, H. Zhu, An sis infection model incorporating media coverage, *Rocky Mt. J. Math.*, **38** (2008), 1323–1334.
3. J. Cui, Y. Sun, H. Zhu, The impact of media on the control of infectious diseases, *J. Dyn. Differ. Equ.*, **20** (2008), 31–53.
4. L. Wang, D. Zhou, Z. Liu, D. Xu, X. Zhang, Media alert in an sis epidemic model with logistic growth, *J. Biol. Dynam.*, **11** (2017), 120–137.
5. R. Liu, J. Wu, H. Zhu, Media/psychological impact on multiple outbreaks of emerging infectious diseases, *Comput. Math. Methods Med.*, **8** (2007), 153–164.
6. J. M. Tchuenche, N. Dube, C. P. Bhunu, R. J. Smith, C. T. Bauch, The impact of media coverage on the transmission dynamics of human influenza, *BMC Public Health*, **11** (2011), 1–16.
7. C. Sun,W. Yang, J. Arino, K. Khan, Effect of media-induced social distancing on disease transmission in a two patch setting, *Math. Biosci.*, **230** (2011), 87–95.
8. A. K. Misra, A. Sharma, J. B. Shukla, Modeling and analysis of effects of awareness programs by media on the spread of infectious diseases, *Math. Comput. Model.*, **53** (2011), 1221–1228.
9. A. Wang, Y. Xiao, A Filippov system describing media effects on the spread of infectious diseases, *Nonlinear Anal. Hybr. Syst.*, **11** (2014), 84–97.
10. Y. Xiao, X. Xu,S. Tang, Sliding mode control of outbreaks of emerging infectious diseases, *Bull. Math. Biol.*, **74** (2012), 2403–2422.
11. R. Gallotti, F. Valle, N. Castaldo, Assessing the risks of "infodemics" in response to COVID-19 epidemics, *Nat. Hum. Behav.*, (2020).
12. Y. Zhao, L. Zhang, S. Yuan, The effect of media coverage on threshold dynamics for a stochastic SIS epidemic model, *Phys. A*, **512** (2018), 248–260.
13. A. C. Lowen, J. Steel, Roles of humidity and temperature in shaping in uenza seasonality, *J. Virol.*, **88** (2014), 7692–7695.
14. I. Bashkirtseva, L. Ryashko, Sensitivity analysis of stochastic attractors and noise-induced transitions for population model with allee effect, *Chaos*, **21** (2011), 047514.
15. I. Bashkirtseva, L. Ryashko, Stochastic sensitivity analysis of noise-induced excitement in a prey–predator plankton system, *Front. Life Sci.*, **5** (2011), 141–148.
16. I. Bashkirtseva, L. Ryashko, Stochastic bifurcations and noise-induced chaos in a dynamic prey–predator plankton system, *Int. J. Bifurcat. Chaos*, **24** (2014), 1450109.
17. X. Yu, S. Yuan, Asymptotic properties of a stochastic chemostat model with two distributed delays and nonlinear perturbation, *Discrete Cont. Dyn. B*, **25** (2020), 2373–2390.
18. S. Zhao, S. Yuan, H. Wang, Threshold behavior in a stochastic algal growth model with stoichiometric constraints and seasonal variation, *J. Differ. Equations*, **268** (2020), 5113–5139.

19. X. Yu, S. Yuan, T. Zhang, Asymptotic properties of stochastic nutrient-plankton food chain models with nutrient recycling, *Nonlinear Anal.-Hybri.*, **34** (2019), 209–225.

20. C. Xu, S. Yuan, T. Zhang, Average break-even concentration in a simple chemostat model with telegraph noise, *Nonlinear Anal.-Hybri.* **29** (2018), 373–382.

21. C. Xu, S. Yuan, Competition in the chemostat: A stochastic multi-species model and its asymptotic behavior, *Math. Biosci.*, **280** (2016), 1–9.

22. C. Xu, S. Yuan, T. Zhang, Competitive exclusion in a general multi-species chemostat model with stochastic perturbations, *Bull. Math. Biol.*, DOI: 10.1007/s11538-020-00843-7.

23. Y. Zhao, S. Yuan, J. Ma, Survival and stationary distribution analysis of a stochastic competitive model of three species in a polluted environment, *Bull. Math. Biol.*, **77** (2015), 1285–1326.

24. D. Wu, H. Wang, S. Yuan, Stochastic sensitivity analysis of noise-induced transitions in a predator-prey model with environmental toxins, *Math. Biosci. Eng.*, **16** (2019), 2141–2153.

25. C. Xu, S. Yuan, T. Zhang, Stochastic sensitivity analysis for a competitive turbidostat model with inhibitory nutrients, *Int. J. Bifurcat. Chaos*, **26** (2016), 707–723.

26. L. Gammaitoni, P. Jung, F. Marchesoni, Stochastic resonance, *Rev. Mod. Phys.*, **70** (1998), 223.

27. W. Horsthemke, Noise induced transitions, *Non-Equi. Dyna. Chem. Sys.*, (1984), 150–160.

28. K. Matsumoto, I. Tsuda, Noise-induced order, *J. Stat. Phys.*, **31** (1983), 87–106.

29. J. Gao, S. Hwang, J. Liu, When can noise induce chaos? *Phys. Rev. Lett.*, **82** (1999), 1132–1135.

30. M. A. Zaks, X. Sailer, L. S. Geier, A. Neiman, Noise induced complexity: From subthreshold oscillations to spiking in coupled excitable systems, *Chaos*, **15** (2005), 026117.

31. S. Kim, S. H. Park, C. S. Ryu, Colored-noise-induced multistability in nonequilibrium phase transitions, *Phys. Rev. E*, **58** (1998), 7994-7997.

32. S. L. Souza, A. M. Batista, I. L. Caldas, R. L. Viana, T. Kapitaniak, Noise-induced basin hopping in a vibro-impact system, *Chaos Soliton. Fract.*, **32** (2007), 758–767.

33. M. I. Dykman, R. Mannella, P. V. E. McClintock, N. Stocks, Fluctuation-induced transitions between periodic attractors: Observation of supernarrow spectral peaks near a kinetic phase transition, *Phys. Rev. Lett.*, **65** (1990), 48–51.

34. S. Yuan, D. Wu, G. Lan, H. Wang, Noise-induced transitions in a nonsmooth producer-grazer model with stoichiometric constraints, *Bull. Math. Biol.*, **82** (2020), 55.

35. S. Kraut, U. Feudel, Multistability, noise, and attractor hopping: The crucial role of chaotic saddles, *Phys. Rev. E*, **66** (2002), 015207.

36. I. Bashkirtseva, L. Ryashko, I.Tsvetkov, Sensitivity analysis of stochastic equilibria and cycles for the discrete dynamic systems, *Dyna. Cont. Dis. Imp. Syst.*, **17** (2010), 501–515.

37. I. Bashkirtseva, T. Ryazanova, L. Ryashko, Confidence domains in the analysis of noiseinduced transition to chaos for Goodwin model of business cycles, *Int. J. Bifurc. Chaos*, **24** (2014), 1440020.

AIMS Press